Available online at www.sciencedirect.com
ScienceDirect
Journal of Power Sources 164 (2007) 809–814
JOURNAL OF POWER SOURCES
www.elsevier.com/locate/jpowsour

Short communication

CO_X-free H_2 production via catalytic decomposition of CH_4 over Ni supported on zeolite catalysts

J. Ashok, S. Naveen Kumar, A. Venugopal, V. Durga Kumari, M. Subrahmanyam *

Indian Institute of Chemical Technology, Hyderabad 500007, India

Received 9 October 2006; received in revised form 21 November 2006; accepted 21 November 2006
Available online 2 January 2007

Abstract

Catalytic decomposition of methane produces CO_X-free hydrogen, which is necessary for PEM fuel-cell applications. In this paper, hydrogen production by catalytic decomposition of methane at 550 °C over Ni on HY, USY, SiO_2 and SBA-15 supports is examined at atmospheric pressure. The catalytic activities and the life times of the catalysts are evaluated and discussed. The relationships between catalyst performance and characterization of the fresh and used catalysts are discussed with the results obtained from SEM, XRD, TPR, solid acidity and the measured carbon contents generated of the used samples along with their H_2 production rates. Among all the catalysts tested, Ni supported on HY zeolite showed a higher activity of 955 mol H_2 (mol Ni)$^{-1}$ and a longevity of 720 min at 550 °C.

Keywords: Methane decomposition; Carbon filaments; Zeolites; SBA-15; Hydrogen production

1. Introduction

Hydrogen may become a renewable and sustainable energy carrier of the future [1,2]. There are several processes for the production of hydrogen and two of them are: steam and auto thermal reforming of natural gas. Although these processes are mature technologies, they are somewhat complex and involve multiple steps. In addition, H_2 is required without CO, which poisons the Pt electrode of fuel cells. To overcome these problems, the direct conversion of methane to pure hydrogen is the most challenging subject [3–11].

Nickel is a common transition metal used for the decomposition, by steam reforming, and/or partial oxidation of methane [8–16]. The most important factors that influence the carbon deposits during methane decomposition are the particle size, dispersion and stabilization of the metallic nickel particles by selecting appropriate support. Takenaka et al. [12] reported that a typical 40% Ni/SiO_2 catalyst with the nickel particle size of 60–100 nm that could give the carbon yield of as high as 491 g C (g Ni)$^{-1}$ during methane decomposition at 500 °C. Furthermore, Ermakova et al. [13] reported the 90 wt% Ni/SiO_2 catalyst with the nickel particle of 10–40 nm size provided carbon yields in the order of 385 g C (g Ni)$^{-1}$ at 550 °C. Other supports, such as TiO_2, MgO, ZrO_2 and Al_2O_3 gave relatively lower carbon yields [14]. The 75% Ni–15% Cu–Al_2O_3 catalysts with the nickel particle size of 27 nm gave carbon of 700 g C (g Ni)$^{-1}$ at 625 °C [15]. However, the decomposition of methane led to the formation of traceable CO via the reaction of carbonaceous residues with the oxygen in the support systems like SiO_2 and Al_2O_3 [5,17]. The support materials play a critical role in determining both the methane conversion and CO formation during the decomposition.

In this study, Ni-supported catalysts on USY, HY, SBA-15 and SiO_2 are examined for comparison. The HY supported Ni catalyst showed a higher activity than the other supported catalysts tested. The correlation between the characteristics of the zeolite supports and others along with the catalytic performance were examined with SEM, XRD, TPR, solid acidity measurements and a carbon elemental analysis. The catalytic decomposition of methane (CDM) activities were performed at 550 °C temperature.

2. Experimental

Among the several reported methods for preparing (30 wt%) Ni-supported catalysts, the incipient wetness impregnation

* Corresponding author. Tel.: +91 40 27193165; fax: +91 40 27160921.
E-mail address: Subrahmanyam@iict.res.in (M. Subrahmanyam).

0378-7753/$ – see front matter © 2006 Elsevier B.V. All rights reserved.
doi:10.1016/j.jpowsour.2006.11.029

method was selected. Nickel nitrate $Ni(NO_3)_2{\cdot}6H_2O$ was the source for nickel. USY, HY, SBA-15 and SiO_2 were utilized as catalytic supports. The zeolite supports were commercially available; USY (surface area = 600 $m^2\,g^{-1}$, Si/Al = 2.6, Na_2O = 4 wt%) supplied by Engelhard Corporation, HY (surface area = 500 $m^2\,g^{-1}$, Si/Al = 2.6) supplied by P Q Corporation, USA and SiO_2 (surface area = 500 $m^2\,g^{-1}$, pore volume = 0.75 $cm^3\,g^{-1}$, average pore diameter = 60 Å) from Aldrich were used.

SBA-15 synthesized is as reported earlier in the literature [18] using tetra ethyl orthosilicate (TEOS) and three-block copolymer poly(ethylene glycol)–*block*–poly(propylene glycol)–*block*–poly(ethylene glycol) $EO_{20}PO_{70}EO_{20}$ was the template agent. $EO_{20}PO_{70}EO_{20}$ was dissolved in HCl and homogenized before the addition of H_2O and TEOS. The mixture was stirred for 20 h, and transferred into a Teflon-lined autoclave, which was kept at 100 °C for 24 h. The resulting white solid was filtered, washed with distilled water and dried in a vacuum at room temperature and the resulting white solid was calcined at 500 °C for 6 h.

In a typical impregnation method the required amount of nickel nitrate [$Ni(NO_3)_2{\cdot}6H_2O$] was taken to give Ni loading of 30 wt% with known amount of water in a 100 ml beaker and mixed with the requisite amount of support material to yield the respective Ni wt% needed. These solutions were dried with constant stirring at 100 °C until the sample gets dried and then kept for drying at 100 °C for about 24 h, followed by calcination in air at 600 °C for 5 h. Thus, prepared catalysts were used for evaluating CDM activities.

The catalytic activities were performed at 550 °C at atmospheric pressure in a fixed-bed vertical quartz reactor (i.d. = 0.8 cm, length = 46 cm), operated in a down flow mode heated by an electric furnace. Methane supplied by Vadilal gases limited (99.99%) was used directly without further purification. Many of the experimental conditions used were as reported earlier [8–10] and some of the details were: a catalyst charge of 50 mg, a methane flow rate = 20 ml min^{-1}, a helium flow rate = 40 ml min^{-1}, i.e. GHSV of 72.0 L (h g catalyst)$^{-1}$. Prior to the reaction, the catalyst was reduced at 450 °C with 5% H_2 in N_2 for 2 h. The reaction was continued until all the catalysts were deactivated. Then, obtained catalysts were weighed before and after each experiment. The outflow gas was analyzed by gas chromatography equipped with a carbosphere column and TCD detector using N_2 as a carrier. The conversion of methane was determined using calibrated data. The first analysis was done 5 min after methane was flowed over the catalyst.

The morphology of the catalyst before and after reaction was recorded by scanning electron microscopy (SEM) of JEOL-JSM 5600 instrument. X-ray diffraction (XRD) patterns of all the samples were obtained on a Rigaku miniflex X-ray diffractometer using Ni filtered Cu Kα radiation (λ = 1.5406) from 2θ = 2–80°, at a scan rate of 2° min^{-1}, with the beam voltage and a beam current of 30 kV and 15 mA, respectively. The reducibility of the NiO present in catalysts calcined at 600 °C were studied by temperature programmed reduction (TPR) [9,10]. About 50 mg of catalyst sample was loaded in an isothermal zone of the reactor and heated at a rate of 10 °C min^{-1} to 450 °C in 30 $cm^3\,min^{-1}$ helium gas which facilitated desorption of the physically adsorbed water. After the sample was cooled to room temperature, the helium was switched to 20 $cm^3\,min^{-1}$ of reducing gas consisting of 5% H_2 in argon and the temperature was increased to 700 °C at a rate of 5 °C min^{-1}. The reactor effluent gas was passed through a molecular sieve trap to remove the produced water and was analyzed by gas chromatography (GC) using a thermal conductivity detector (TCD).

The acidic strength of the solid samples was measured by the potentiometric titration method. A known mass of solid suspended in acetonitrile was stirred for 3 h and then the suspension was titrated with a solution of 0.05N *n*-butylamine in acetonitrile at a flow rate of 0.05 ml min^{-1}. The variation in the electrode potential was measured in a microprocessor-based automatic titrator (Schott, Germany). The carbon analysis data was collected with VARIO EL analyser instrument. The surface area of the support materials was measured by N_2 physical adsorption at 77 K in an Autosorb-I (Quantachrome) instrument. The specific surface area was calculated by applying the BET method.

3. Results and discussions

3.1. CDM activities

Catalytic activity runs were performed in a fixed-bed microreactor over Ni/HY, Ni/USY, Ni/SiO_2 and Ni/SBA-15 catalysts. The reactions were performed at 550 °C and the loading of Ni was adjusted to 30 wt% [9]. All the experiments performed under similar conditions were to know the influence of the support materials. Carbon and hydrogen were regarded as the only products of methane decomposition and no liquid products were seen. The following reaction occurs during the process:

$$CH_4 \rightarrow C + 2H_2 \quad \Delta H^\circ = 75.6\,\text{kJ mol}^{-1}$$

Fig. 1 represents the change in methane conversion with time on stream until complete deactivation of the catalysts.

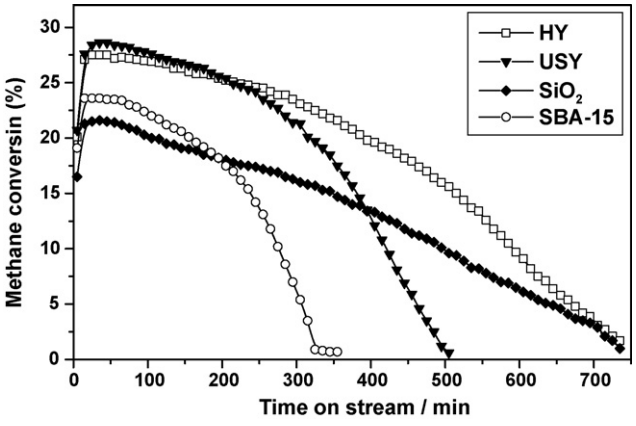

Fig. 1. Methane conversion during CDM over 30 wt% Ni supported catalysts at 550 °C as a function of time.

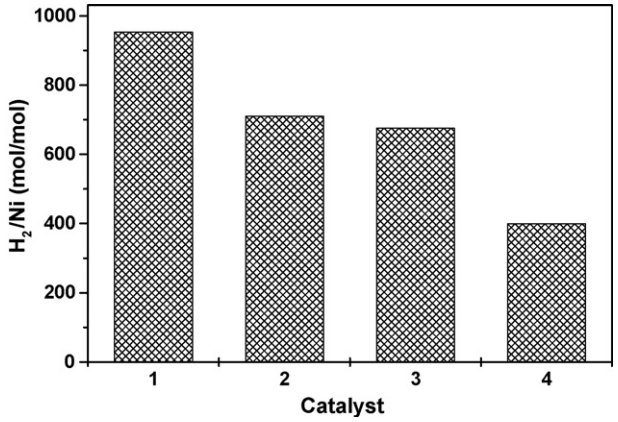

Fig. 2. Hydrogen yields during methane decomposition over 30 wt% Ni supported (1) HY, (2) USY, (3) SiO_2 and (4) SBA-15 catalysts at 550 °C.

Among all the catalysts tested the Ni/HY catalyst was found to have a higher activity compared to other catalysts. The total run time increased over the catalyst supports in the order of HY ∼ SiO_2 > USY > SBA-15. On the other hand, the overall accumulation of carbon was in the order of HY > USY > SiO_2 > SBA-15.

The methane conversion was generally found to be high in the initial stages and decreased due to carbon deposition rapidly or gradually with time on stream until the catalyst was finally deactivated as a result of carbon deposition. The carbon deposited on the surface covered the active sites or accumulated at the entrance of the pores to block further access of the reactants. This aspect was verified by XRD analysis and the carbon content estimations that were performed over the deactivated catalysts which were removed from the reactor after each run.

Fig. 2 shows the moles of hydrogen formed per mole of nickel (H_2/Ni) of the catalyst after complete deactivation. The carbon yields were denoted as C/Ni (moles of carbon deposited per mole of nickel (Ni)) and this corresponded to a half of H_2/Ni mole ratio. The yields were estimated from the kinetic curves of the methane conversion and they are shown in Fig. 1, assuming that methane decomposition to carbon and hydrogen proceeded stoichiometrically. The high hydrogen yield (955 mol (mol Ni)$^{-1}$) for Ni/HY catalyst corroborated the sustainability and longevity compared to other systems tested. An experimental error of the order of ±5 in activity evaluation studies was noted during the evaluation.

Table 1 provides a summary of all the experiments conducted along with the total run time, Ni crystallite size, H_2 yields, solid acidic strengths and H_2 uptakes (from TPR). Ni crystallite sizes were calculated from the XRD results obtained for the reduced catalysts using the Scherer equation [9,10]. It is found that along with many factors, the size of Ni crystal also influenced the activity of methane decomposition. Furthermore, Ni/HY showed longevity and a C/Ni (mol mol^{-1}) ratio of value 478 mol mol^{-1} for a crystallite size of Ni 18 nm.

3.2. XRD analysis

Fig. 3 shows fresh and deactivated Ni supported over HY, USY, SiO_2 and SBA-15 catalysts. In Fig. 3(a) the reflections at $2\theta = 37.28°$, 43.3°, 62.9 and 75.3° and their major corresponding '*d*' values, 2.09, 1.48, 2.41 are attributed to the presence of a crystalline NiO phase [ICDS No.: 01-1239] as seen from the patterns of fresh catalysts. The NiO phase in the fresh catalysts suggests the decomposition of nickel nitrate in air at 600 °C for 5 h to form the NiO species during the preparation of catalysts. However, the patterns of the used catalysts (Fig. 3(b)) with reflections at $2\theta = 26.28°$, 45.2°, 53.9° and 77.0° and their corresponding '*d*' values of 3.38, 2.00, 1.69 and 1.23 are attributed to graphitic carbon [ICDS No.: 01-0640]. The phase due to metallic Ni and its reflections at $2\theta = 44.4°$, 51.8° and 76.4° and the corresponding '*d*' values 2.03, 1.76, 1.24 also appeared in the patterns of used catalysts [ICDS No.: 04-0850]. The reflections due to SiO_2 and SBA-15 phase could not be seen in fresh and used patterns because of the amorphous nature. On the other hand, the phases corresponding to HY and USY zeolites were clear in Fig. 3(a(1) and (2)) patterns and these do not appear as clear in the used samples Fig. 3(b(1) and (2)) which may be due to the deposition of graphitic carbon. The irreversible carbon that is deposited on the catalyst as proven from the XRD pattern of the deactivated catalysts, indicates that methane decomposition is producing hydrogen and carbon only. The presence of only metallic nickel in the deactivated catalysts reveals that the NiO phase is reduced to form metallic Ni during the pretreatment of the catalyst. It appears that the metallic nickel is active for the decomposition of methane. From this, it is concluded that only a NiO phase is present in the fresh catalysts. On the other hand the deactivated catalysts displayed phases due to both metallic nickel and graphitic carbon too.

3.3. Temperature programmed reduction

The TPR profiles of Ni supported HY, USY, SiO_2 and SBA-15 are shown in Fig. 4. The shape of TPR pattern is affected

Table 1
Summary of the experiments conducted

Catalyst	Run time (min)	Ni crystallite size	H_2 yield (mol mol^{-1})	Acidic strength E_i (mV)	H_2 uptakes (mmol g^{-1})[a]
HY	720	18	955	173	4.6
USY	515	20	712	110	4.5
SiO_2	720	21	677	158	5.0
SBA-15	400	24	400	255	5.6

[a] H_2 uptakes were calculated from TPR profiles.

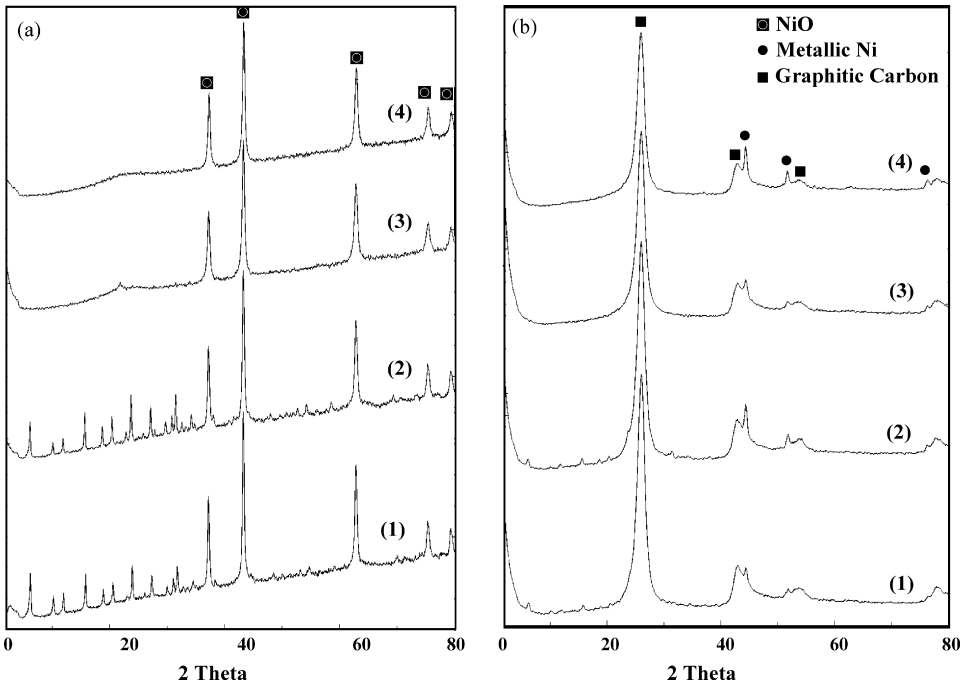

Fig. 3. XRD patterns of (a) fresh and (b) used 30 wt% Ni supported over (1) HY, (2) USY, (3) SiO_2 and (4) SBA-15 catalysts.

by the particle size distribution of the reacting solid. The occurrence of multiple peaks may be expected in case of multi-modal distributions for which separate knowledge of the particle size distribution is of considerable help for the correct interpretation of TPR profiles. The size of the particles is sensitive to TPR measurements and data is not providing straightforward information [19].

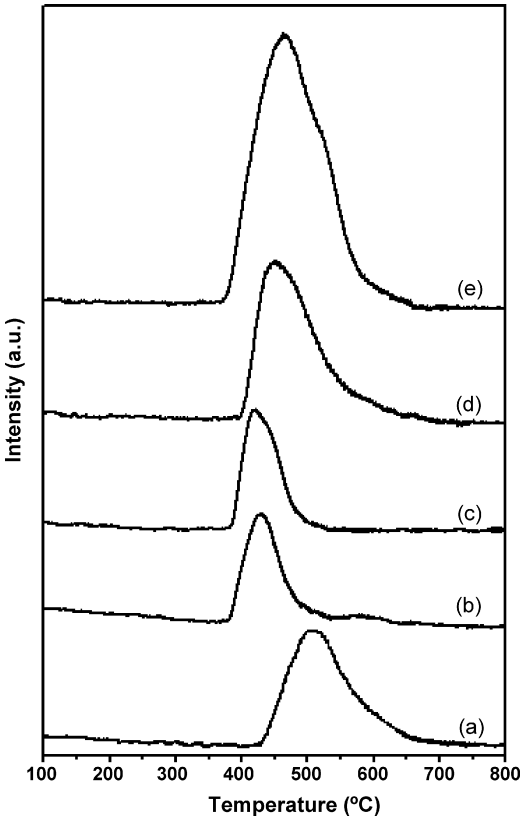

Fig. 4. TPR profiles of 30 wt% Ni supported (a) HY, (b) USY, (c) SiO_2, (d) SBA-15 and (e) NiO catalysts.

It is clearly evident from the patterns that the Ni catalysts exhibit a very different reduction behavior. The maximum temperatures for large peak areas are 506, 428, 419 and 451 °C for HY, USY, SiO_2 and SBA-15, respectively. All the catalysts show single reduction peaks except for the USY zeolite. This shows two reduction peaks, one is a low temperature peak observed at 428 °C and there is a small high temperature peak at 577 °C. The H_2 uptakes are shown in Table 1 and they are 4.6, 4.5, 5.0 and 5.6 mmol g^{-1} for Ni supported on HY, USY, SiO_2 and SBA-15, respectively. It is reported that the reduction of nickel bulk oxide occurs at 300–400 °C and the sample attached to silica found to have at 400–500 °C temperatures [20]. The XRD analysis of fresh catalysts revealed the presence of only a NiO phase. No phase is attributed to Ni_2O_3 in any of the catalysts. The reduction peak for Ni_2O_3 usually appears at 250 °C for the nickel supported silica catalysts [12] and is not seen in the present systems. The TPR analysis of the reference bulk NiO was performed for comparison purposes. It showed a single reduction signal centered at 460 °C. The reduction of bulk Ni (II) species occured at 400 °C and from this it was concluded that bulk NiO species was present on the catalyst and it was also complimented by the XRD data of fresh catalyst samples.

3.4. SEM analysis

The SEM micrographs of fresh and used Ni supported HY, USY, SiO_2 and SBA-15 catalysts are shown in Fig. 5. The images were measured after the reaction because of a large amount of carbon deposited on the catalysts during methane

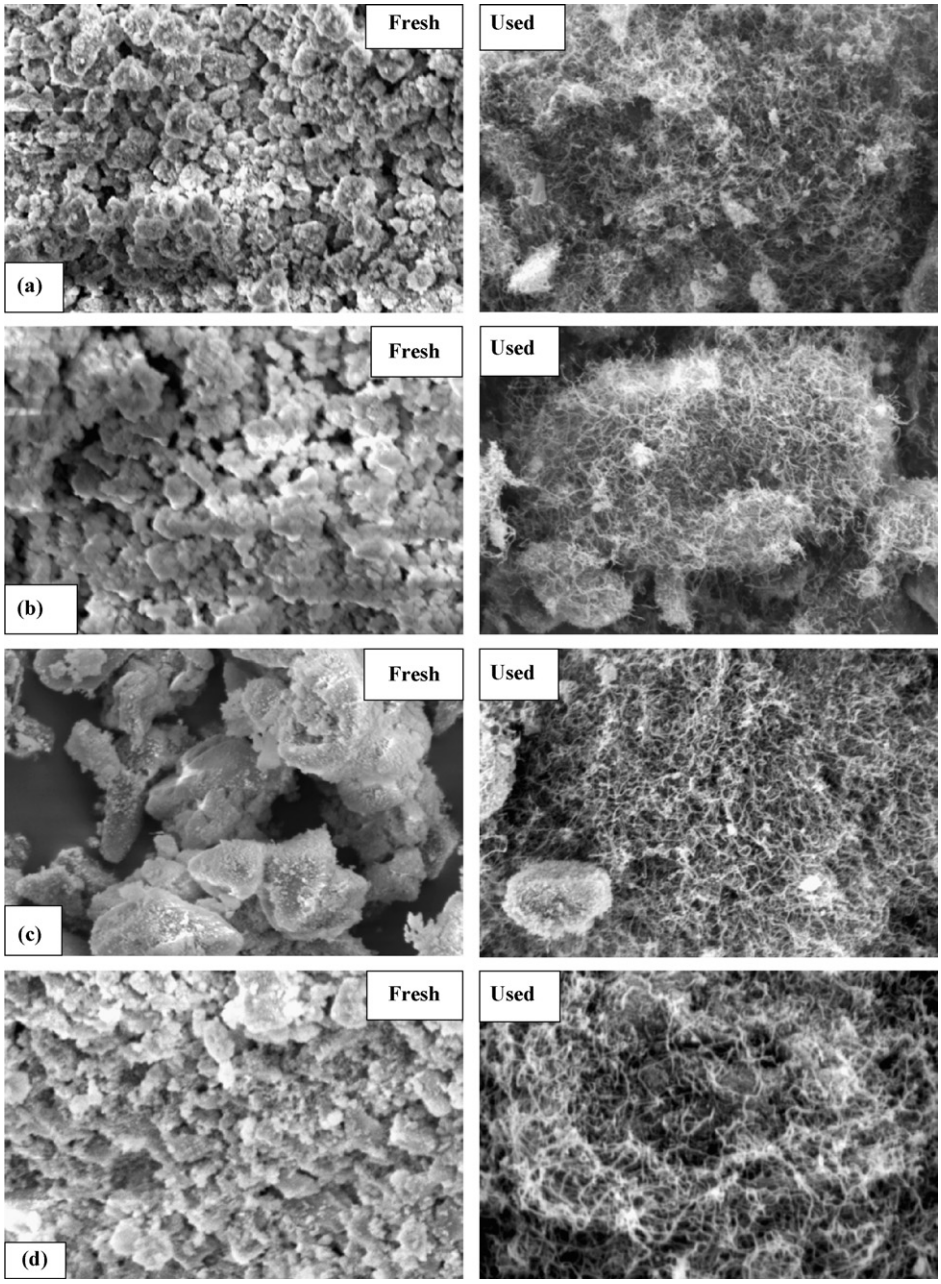

Fig. 5. SEM images of fresh and used 30 wt% Ni supported (a) HY, (b) USY, (c) SiO_2 and (d) SBA-15 catalysts.

decomposition at 550 °C. It is seen that deposited carbon over all the catalysts are a whisker type of nanofilament. However, the diameter and lengths of the carbon nanofilaments are different. Furthermore, the graphitic nature of filamentous carbon is evident from XRD analysis. In the catalytic decomposition of methane to hydrogen, in order to maintain a high catalytic activity and a long lifetime, whisker or fiber types of carbon formation over active species are required. In contrast, low catalytic activities are the result of rapid carbon deposition on the catalyst's active sites. Another different feature in the SEM images is the abundance of bright areas that are associated with a bare Ni surface and the amount of this exposed Ni is substantially lower in the deactivated samples. From Fig. 5, a Ni metal particle at the tip of the carbon nanofiber, decomposes methane to grow carbon nanofibers and the diameter of a carbon nanofiber had the same size as that of the Ni metal particle at the tip. This is in agreement with earlier reports [9,10].

3.5. Acidity of the catalysts

Fig. 6 shows the potentiometric titration curves obtained for various Ni supported catalysts, where the electrode potential is shown as a function of *n*-butylamine (mequiv. (g catalyst)$^{-1}$). These potentiometric curves show initial electrode potentials of 173, 110, 158 and 255 mV for Ni supported HY, USY,

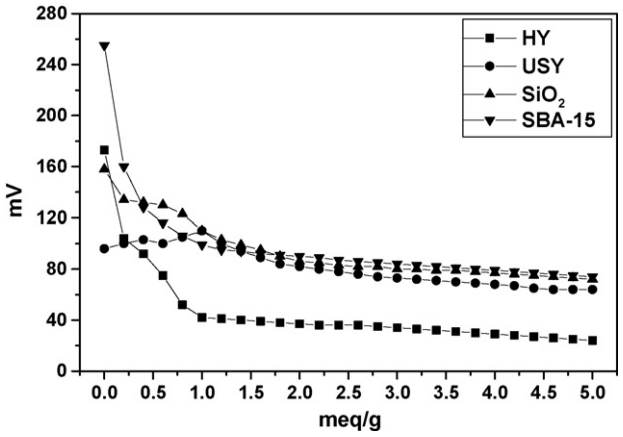

Fig. 6. Potentiometric titration profiles of 30 wt% Ni supported catalysts.

SiO_2 and SBA-15, respectively. This method enables us to determine the total number of acidic sites and their strength. It is suggested that the initial electrode potential (E_i) represents the maximum acid strength of the sites and the value (mequiv. amine (g catalyst)$^{-1}$) where plateau reached indicates the total number of acidic sites [21]. The acid strength has been classified according to the following scale: $E_i > 100$ mV (very strong sites); $0 < E_i < 100$ mV (strong sites); $-100 < E_i < 0$ mV (weak sites) and $E_i < -100$ mV (very weak sites). The acidic strengths of all the catalysts are shown in Table 1. It seems that all the catalysts exhibit very strong acidic strengths as they showed higher E_i values which are found to vary in the range 110–255 mV. The acidic strength of the supports decreased in the following order: SBA-15 > HY > SiO_2 > USY. Inaba et al. [16] reported that the amount of ammonia desorbed from zeolite support was inversely proportional to the C/Ni value and is in good agreement with our results obtained for SiO_2 and SBA-15 supported systems (Fig. 1). On the other hand, Ni supported HY showed higher activity than USY support and the lower activity of USY over HY was due to the presence of 4% Na_2O. It is suggested that the amount of molar acidity of the catalysts also has effect on methane decomposition activity.

3.6. Carbon analysis

All the deactivated catalysts were recovered in an inert gas and subsequently estimated for carbon contents using elemental analyses. The XRD analysis of the deactivated catalysts revealed the presence of graphitic carbon. It is evident from Table 1 that the activity and the longevity of the catalyst can be correlated with the amount of carbon deposited. However, in this investigation the 30 wt% Ni/HY showed the highest CDM activity and longevity even though all the catalysts were found to have the same amount of carbon deposition. The irreversibility of the reaction is further confirmed by TPR analysis of the deactivated catalyst that could not display any reduction profile due to hydrogasification, i.e. carbon hydrogenation even up to 650 °C.

4. Conclusions

In summary, 30 wt% Ni supported over HY, USY, SBA-15 and SiO_2 catalysts were tested for methane decomposition at 550 °C. The activity towards methane decomposition depended on certain parameters such as; temperature, nature of the support material, type and amount of the active metal. The supported catalysts were characterized with SEM, XRD, TPR and also by acidity measurements. It is apparent that the size of Ni metal and solid acidity of the catalyst influenced the activity of the methane decomposition. The 30 wt% Ni/HY catalyst demonstrated superior activity and longevity producing a H_2 yield of 995 mol (mol Ni)$^{-1}$ compared to other Ni supported catalysts. Finally, it was found that the use of HY and USY zeolite supports were found to be suitable for the catalytic decomposition methane.

Acknowledgements

The authors thank CSIR, New Delhi for funding this project under NMITLI (TLP-0008) program and Dr. A Ratnamala for providing SBA-15 sample.

References

[1] R. Aiello, J.E. Fiscus, H.C. zur Loye, M.D. Amiridis, Appl. Catal. A 192 (2000) 227.
[2] M. Subrahmanyam, V. Durga Kumari, K.B.S. Prasad, National Seminar on Fuel Cell-Materials Systems and Accessories, Ambernath, September, 2003, p. 128.
[3] M.G. Poirier, C. Sapundzhiev, Int. J. Hydrogen Energy 22 (1997) 429.
[4] Steinfeld, V. Kirillov, G. Kuvshinov, Y. Mogilnykh, A. Reller, Chem. Eng. Sci. 52 (1997) 3599–3603.
[5] T.V. Choudhary, C. Sivadinarayana, C.C. Chusuei, A. Klinghoffer, D.W. Goodman, J. Catal. 199 (2001) 9.
[6] M. Serban, M.A. Lewis, C.L. Marshall, R.D. Doctor, Energy Fuels 17 (2003) 705.
[7] N. Muradov, Energy Fuels 12 (1998) 41.
[8] J. Ashok, S. Naveen Kumar, A. Venugopal, V. Durga Kumari, S. Tripathi, M. Subrahmanyam, Catal. Commun., submitted for publication.
[9] A. Venugopal, J. Ashok, S. Naveen Kumar, V. Durga Kumari, M. Subrahmanyam, Int. J. Hydrogen Energy, in press.
[10] A. Venugopal, J. Ashok, S. Naveen Kumar, V. Durga Kumari, M. Subrahmanyam, Fuel, submitted for publication.
[11] J. Ashok, S. Naveen Kumar, A. Venugopal, K.B.S. Prasad, V. Durga Kumari, M. Subrahmanyam, V.V.D.N. Prasad, P. Pal, M.O. Garg, National Workshop on Catalysis for Energy at BHU, Varanasi, India, February, 2006.
[12] S. Takenaka, S. Kobayashi, H. Ogihara, K. Otsuka, J. Catal. 217 (2003) 79.
[13] M.A. Ermakova, D.Yu. Ermakova, G.G. Kuvshinov, L.M. Plyasova, J. Catal. 187 (1999) 77–84.
[14] J. Li, G. Lu, K. Li, W. Wang, J. Mol. Catal. A 221 (2004) 105.
[15] T.V. Reshetenko, L.B. Avdeeva, Z.R. Ismagilov, A.L. Chuvilin, V.A. Ushakov, Appl. Catal. A 247 (2003) 51.
[16] M. Inaba, K. Murata, M. Saito, I. Takahara, N. Mimura, React. Kinet. Catal. Lett. 77 (2002) 109–115.
[17] P.F. Aparicio, A.G. Ruiz, Appl. Catal. A 148 (1997) 343.
[18] D. Zhao, J. Feng, Q. Huo, N. Melosh, G.H. Fredrickson, B.F. Chmelka, G.D. Stucky, Science 279 (1998) 548.
[19] B. Mile, D. Stirling, M.A. Zammitt, A. Lovell, M. Webb, J. Catal. 114 (1998) 217.
[20] S. Takenaka, H. Ogihara, K. Otsuka, J. Catal. 208 (2002) 54.
[21] Ch. Srilakshmi, N. Lingaiah, P. Nagaraju, P.S. Sai Prasad, K.V. Narayana, A. Martin, B. Lucke, Appl. Catal. A 309 (2006) 247.